European Journal of Scientific Research
ISSN 1450-216X / 1450-202X Vol. 150 No 2 September, 2018, pp. 240-251
http://www. europeanjournalofscientificresearch.com

# MHD and Surface Roughness Effects on Couple Stress Fluid between Porous Triangular Plates with Velocity Slip

**S. Sangeetha**
*Department of Mathematics*
*SRM Institute of Science and Technology*
*Kattankulathur-603 203*
E-mail: sangeethasekar@yahoo.com

**Sundarammal Kesavan**
*Department of Mathematics*
*SRM Institute of Science and Technology*
*Kattankulathur-603 203*
E-mail: sundarammal.k@ktr.srmuniv.ac.in

**Abstract**

This theoretical study is about the effect of Magneto hydrodynamic and surface roughness on porous triangular plates with velocity slip lubricated with couple stress fluid. The result signifies that the pressure increases for increasing values of couple stress parameter. But decreases for other parameters. Further the work load decreases due to magnetic effect. Christensen's stochastic theory for rough surface is used to derive the modified Reynolds equation. For pressure, work load and time the closed form expression is obtained.

**Keywords:** Surface roughness, couple stress, velocity slip, MHD, Porous

## 1. Introduction

Numerous problems associated with the motion of a liquid lubricant which is electrically conducted in MHD are given importance. The impact of surface roughness on the squeeze film of porous elliptical plates together with couple stress fluid and traversed magnetic field was studied by Syed Tasneem Fathima et.al [1]. The study of K.C Patel and J.L Gupta [2] reveals that the load capacity is considerably increased by minimizing velocity slip in an inclined porous slider bearing.

It is known from the study of N.B. Naduvinamani [3] that the work load is enhanced by using the magnetic effect. In non-Magnetic case the squeeze time is lengthened compared to magnetic for porous circular stepped plates. The Fourier Bessel series is used to get the pressure for porous transversely triangular plates using couple stress fluid and also for the porous transversely circular plates in the analysis of Sundarammal Kesavan et.al [4] [5]. The MHD with couple stress for triangular plates is obtained by Birdar Kashinath [6]. Bujurke NM et al [7] have analyzed that for finite rectangular plates the numerical solutions are derived when the negatively skewed surface roughness pattern enhances work load and non- dimensionless time.

Sundarammal Kesavan [8] derived the time-height relationship by Runge-kutta's fourth order in MHD for finite rectangular plates with rough surface. The hydro magnetic squeeze films for porous rectangular plates using velocity slip at the porous region by using Beavers-Joseph condition [9]. Ramesh B. Kunenatti [10] derived in their analysis that use of finite difference-based multigrid method for finite rectangular plates [11] Dhanapal P. Basti used the Christensen concept to analyzed the roughness on curved Annular Plates. The numerical results for rough surface on porous step-slider bearing shows that negatively skewed roughness enhances the load and decreases for frictional force by N.B. Naduvinamani and A. Siddagouda [12]. The couple stress fluid with MHD and rough surface on porous triangular plates with velocity slip using Beaver's Joseph criteria [13].

## 2. Mathematical Formulation

**Figure 1:** Configuration of the Squeeze Film bearing system

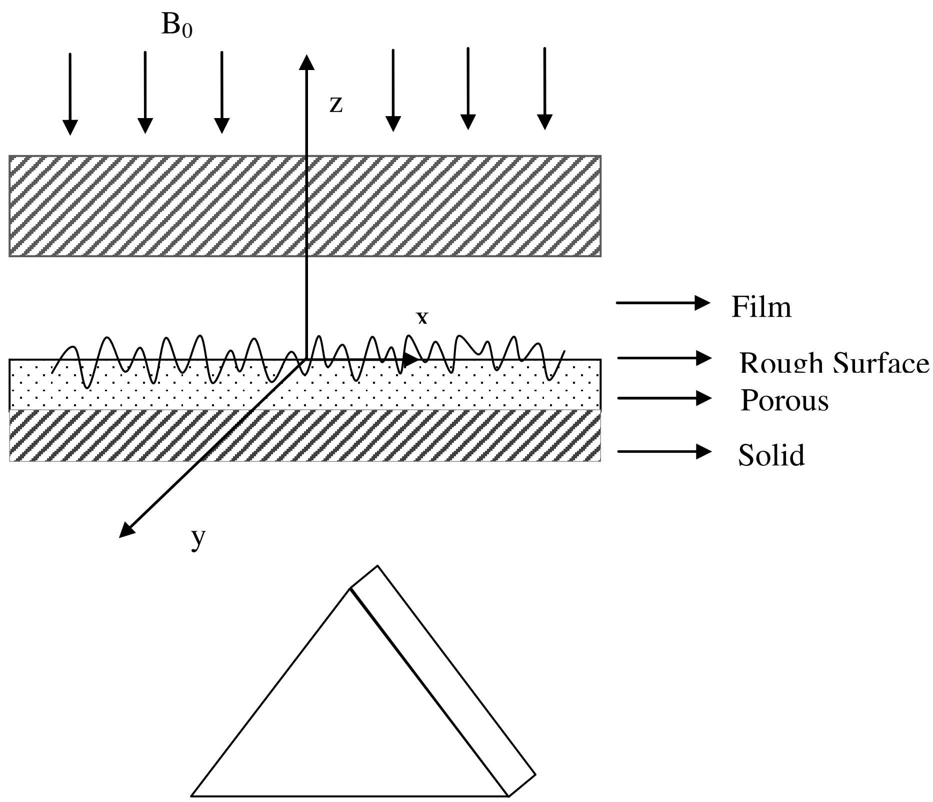


Two triangular plates moving towards one another with normal velocity (which is assumed to be rough at Z=0) as shown in fig.1. Also, to these plates the uniform magnetic field $B_o$ is perpendicularly applied. It is assumed that the lubrication in the film region is considered to be an incompressible stokes [15] couple stress fluid in which body force and body couples are absent. The above assumptions are made along with the hydro-dynamic lubrication and hydro- magnetic lubrication is made to thin films [16] the MHD equations for the couple stress fluid are

$$\mu \frac{\partial^2 u}{\partial z^2} - \eta \frac{\partial^4 u}{\partial z^4} - \sigma B_o^2 u = \frac{\partial p}{\partial x} \tag{1}$$

$$\mu \frac{\partial^2 v}{\partial z^2} - \eta \frac{\partial^4 v}{\partial z^4} - \sigma B_o^2 v = \frac{\partial p}{\partial y} \tag{2}$$

$$\frac{\partial p}{\partial z} = 0 \tag{3}$$

$$\frac{\partial u}{\partial x}+\frac{\partial v}{\partial y}+\frac{\partial w}{\partial z}=0 \tag{4}$$

The boundary conditions for velocity components are

(i) At the upper surface (z=H)

$$u=v=0\,,\frac{\partial^2 u}{\partial z^2}=\frac{\partial^2 v}{\partial z^2}=0 \tag{5a}$$

$$w=\frac{\partial H}{\partial t} \tag{5b}$$

(ii) At the upper surface (z = 0)

$$\frac{\alpha}{\sqrt{k}}(u-u^*)=\frac{\partial u}{\partial z} \tag{6a}$$

$$\frac{\alpha}{\sqrt{k}}(v-v^*)=\frac{\partial v}{\partial z} \tag{6b}$$

$$w=w^* \tag{6c}$$

$$\frac{\partial^2 u}{\partial z^2}=\frac{\partial^2 v}{\partial z^2}=0 \tag{7}$$

By applying modified Darcy's law in the flow of couplestress fluid between the porous region with magnetic field is given by,

$$u^*=\frac{-k}{\mu\left(1-\beta+\left(k\sigma B_o^2/\mu M'\right)\right)}\frac{\partial p^*}{\partial x} \tag{8a}$$

$$v^*=\frac{-k}{\mu\left(1-\beta+\left(k\sigma B_o^2/\mu M'\right)\right)}\frac{\partial p^*}{\partial y} \tag{8b}$$

$$w^*=\frac{k}{\mu(1-\beta)}\frac{\partial p^*}{\partial z} \tag{8c}$$

The pressure p* in the porous region satisfies the Laplace equation

$$\frac{\partial^2 p^*}{\partial x^2}+\frac{\partial^2 p^*}{\partial y^2}+\left(\frac{1-\beta+\left(k\sigma B_o^2/\mu M'\right)}{1-\beta}\right)\frac{\partial^2 p^*}{\partial z^2}=0 \tag{9}$$

Solving the equation (1) and (2) using the boundary condition (5a), (6a) and (7) we obtained the solution as

$$u=\frac{1}{\left(A^2-B^2\right)}\frac{1}{\sigma B_o^2}\frac{\partial p}{\partial x}\left[f_1\left(\frac{B^2\sinh\left(A(z-H)/l\right)}{\sin AH/l}-\frac{A^2\sinh\left(B(z-H)/l\right)}{\sin BH/l}\right)-f_2\right] \tag{10}$$

Where $l=\left(\frac{\eta}{\mu}\right)^{\frac{1}{2}}$ is the Couple stress parameter

$$A=\left\{\frac{1+\left(1-4l^2\frac{\sigma B_o^2}{\mu}\right)^{\frac{1}{2}}}{2}\right\}^{\frac{1}{2}}\quad B=\left\{\frac{1-\left(1-4l^2\frac{\sigma B_o^2}{\mu}\right)^{\frac{1}{2}}}{2}\right\}^{\frac{1}{2}}$$

$$f_1=\frac{\left(1-\xi_1\cos ech\left(AH/l\right)+\xi_2\cos ech\left(BH/l\right)\right)-\left(k\sigma B_o^2/\mu\xi_3\right)}{\left(1-\xi_1\coth\left(AH/l\right)+\xi_2\cot h\left(BH/l\right)\right)}$$

$$f_2 = \left( B^2 \sinh\frac{Az}{l} \cos ech \frac{AH}{l} - A^2 \sinh\frac{Bz}{l} \cos ech \frac{BH}{l} + \left(A^2 - B^2\right) \right)$$

$$\xi_1 = \frac{\sigma^* AB^2}{\left(A^2 - B^2\right) l} \quad \xi_2 = \frac{\sigma^* A^2 B}{\left(A^2 - B^2\right) l} \quad \xi_3 = \left( 1 - \beta + \frac{k \sigma B_o^2}{\mu M'} \right)$$

Similarly

$$v = \frac{1}{\left(A^2 - B^2\right)} \frac{1}{\sigma B_o^2} \frac{\partial p}{\partial y} \left[ f_1 \left( \frac{B^2 \sinh\left(A(z-H)/l\right)}{\sin AH/l} - \frac{A^2 \sinh\left(B(z-H)/l\right)}{\sin BH/l} \right) - f_2 \right] \tag{11}$$

Integrating equation (4) using the boundary condition (5b), (6c) and (8c) we obtain the Reynold's equation

$$\frac{\partial^2 p^*}{\partial x^2} + \frac{\partial^2 p^*}{\partial y^2} = \frac{\sigma B_o^2}{g\left(H, \sigma^*, l, B_o\right)} \left\{ \frac{\partial H}{\partial t} + \frac{k}{\mu(1-\beta)} \frac{\partial p^*}{\partial z}\bigg|_{z=0} \right\} \tag{12}$$

Integrating equation (9) withthe boundary condition

$$\frac{\partial p^*}{\partial z}\bigg|_{z=0} = -\delta \left\{ \frac{1-\beta}{\xi_3} \right\} \left( \frac{\partial^2 p^*}{\partial x^2} + \frac{\partial^2 p^*}{\partial y^2} \right) \tag{13}$$

Using (13) in Eq. (12) we obtain

$$\frac{\partial}{\partial x} \left\{ \left( g\left(H, \sigma^*, l, B_o\right) + \frac{k \delta \sigma B_0^2}{\mu \xi_3} \right) \frac{\partial p}{\partial x} \right\} + \frac{\partial}{\partial y} \left\{ \left( g\left(H, \sigma^*, l, B_o\right) + \frac{k \delta \sigma B_0^2}{\mu \xi_3} \right) \frac{\partial p}{\partial y} \right\} = \sigma B_0^2 \frac{\partial H}{\partial t} \tag{14}$$

$$g\left(H, \sigma^*, l, B_o\right) = \frac{l}{\left(A^2 - B^2\right)} \left\{ g_1 * \left( \left[ \frac{B^2}{A} \tanh\left( \frac{AH}{2l} \right) \right] - \left[ \frac{A^2}{B} \tanh\left( \frac{AH}{2l} \right) \right] \right) + \left[ \left(A^2 - B^2\right) \frac{H}{l} \right] \right\}$$

$$g_1 = \frac{\left( 2 - \xi_1 \coth\left( \frac{AH}{2l} \right) + \xi_2 \coth\left( \frac{BH}{2l} \right) \right) - \left( \sigma^{*2} \alpha^2 \sigma B_o^2 \big/ \mu \xi_3 \right)}{1 - \xi_1 \coth\left( \frac{AH}{l} \right) + \xi_2 \coth\left( \frac{BH}{l} \right)}$$

To represent the surface roughness the mathematical expression for film thickness takes the form

$$H = H + h_s\left(x, y, \xi\right)$$

where

$$E(.) = \int_{-\infty}^{\infty} (.) f\left(h_s\right) dh_s \tag{15}$$

The distribution function of the random variable $h_s$ is $f\left(h_s\right)$.In the application of engineering the rough surface is of Gaussian type.

By the Christensen [14] we assume that

$$f\left(h_s\right) = \begin{cases} \frac{35}{32c^7}\left(c^2 - h_s^2\right)^3 & -c \le h_s \le c \\ 0 & elsewhere \end{cases} \tag{16}$$

In general, there are two types of roughness pattern longitudinal and transverse that is assumed to be in x and y - direction. In this paper the roughness structure is assumed to be one dimensional longitudinal roughness, as we rotate the co-ordinate axes the longitudinal and transverse roughness becomes identical.

$$\frac{\partial}{\partial x}\left\{\left(E\left(g\left(H,\sigma^{*},l,B_{o}\right)\right)+\frac{k\delta\sigma B_{0}^{2}}{\mu\xi_{3}}\right)\frac{\partial p}{\partial x}\right\}+\frac{\partial}{\partial y}\left\{\left(\frac{1}{E\left(1\Big/g\left(H,\sigma^{*},l,B_{o}\right)\right)}+\frac{k\delta\sigma B_{0}^{2}}{\mu\xi_{3}}\right)\frac{\partial p}{\partial y}\right\}=\sigma B_{0}^{2}\frac{\partial H}{\partial t} \quad (17)$$

$$G\left(H,\sigma^{*},l,B_{o},c\right)=\begin{cases}E\left[g\left(H,\sigma^{*},l,B_{o}\right)\right] \text{ for longitudinal}\\ E\left[1/g\left(H,\sigma^{*},l,B_{o}\right)\right]^{-1} \text{ for transverse}\end{cases}$$

$$E\left[g\left(H,\sigma^{*},l,B_{o}\right)\right]=\frac{35}{32c^{7}}\int_{-c}^{c}\left(c^{2}-h_{s}^{2}\right)^{3}g\left(H,\sigma^{*},l,B_{o}\right)dh_{s}$$

$$E\left[\frac{1}{g\left(H,\sigma^{*},l,B_{o}\right)}\right]=\frac{35}{32c^{7}}\int_{-c}^{c}\frac{\left(c^{2}-h_{s}^{2}\right)^{3}}{g\left(H,\sigma^{*},l,B_{o}\right)}dh_{s}$$

$$\frac{\partial^{2}E(p)}{\partial x^{2}}+\frac{\partial^{2}E(p)}{\partial y^{2}}=\frac{\sigma B_{0}^{2}dh/dt}{\left(G\left(H,\sigma^{*},l,B_{o},c\right)+\frac{k\delta\sigma B_{0}^{2}}{\mu\xi_{3}}\right)} \quad (18)$$

The boundary condition is $p(x,y)=0$ (19)

The triangular equation is

$$(x-a)\left(x-\sqrt{3y}+2a\right)\left(x+\sqrt{3y}+2a\right)=0$$

The solution of the equation (18) with the condition (19) gives

$$E(p)=-\frac{\sigma B_{0}^{2}dh/dt}{\left(G\left(H,\sigma^{*},l,B_{o},c\right)+\frac{k\delta\sigma B_{0}^{2}}{\mu\xi_{3}}\right)}\left(1-\frac{3x^{2}}{4a^{2}}-\frac{3y^{2}}{4a^{2}}-\frac{x^{3}}{4a^{2}}+\frac{3xy^{2}}{4a^{3}}\right) \quad (20)$$

The dimensionless pressure is of the form

$$p^{*}=\frac{M_{o}^{2}}{9\sqrt{3}}\left\{\frac{\left(1-x^{*}\right)\left(1+\frac{\sqrt{3}y^{*}}{2}+\frac{x^{*}}{2}\right)\left(1-\frac{\sqrt{3}y^{*}}{2}+\frac{x^{*}}{2}\right)}{\left(G\left(H^{*},\mathrm{s},l^{*},\mathrm{M}_{o},\mathrm{C}\right)+\frac{\psi M_{o}^{2}}{\xi_{3}^{*}}\right)}\right\} \quad (21)$$

$$l^{*}=\frac{2l}{h_{o}},\quad H^{*}=\frac{H}{h_{o}},\ x^{*}=\frac{x}{a},\quad M_{o}=B_{o}h_{o}\left(\frac{\sigma}{\mu}\right)^{\frac{1}{2}},\ k=\sigma^{*2}\alpha^{2},\quad y^{*}=\frac{y}{a},s=\frac{\sigma^{*}}{h_{o}},\psi=\frac{k\delta}{h_{o}^{3}},h_{s}^{*}=\frac{h_{s}}{h_{o}},C=\frac{c}{h_{o}}$$

$$A=\left\{\frac{1+\left(1-l^{*2}M_{o}^{2}\right)^{\frac{1}{2}}}{2}\right\}^{\frac{1}{2}};B=\left\{\frac{1-\left(1-l^{*2}M_{o}^{2}\right)^{\frac{1}{2}}}{2}\right\}^{\frac{1}{2}}$$

$$G\left(H^{*},\mathrm{s},l^{*},\mathrm{M}_{o},\mathrm{C}\right)=\frac{l^{*}}{2\left(A^{*2}-B^{*2}\right)}\left\{\begin{array}{l}g_{1}^{*}*\left(\left[\frac{B^{*2}}{A^{*}}\tanh\left(\frac{A^{*}\left(H^{*}+h_{s}^{*}\right)}{l^{*}}\right)\right]-\left[\frac{A^{*2}}{B^{*}}\tanh\left(\frac{A^{*}\left(H^{*}+h_{s}^{*}\right)}{l^{*}}\right)\right]\right)\\+\left[\left(A^{*2}-B^{*2}\right)\frac{2\left(H^{*}+h_{s}^{*}\right)}{l^{*}}\right]\end{array}\right\}$$

$$g_{1}^{*}=\frac{\left(2-\xi_{1}^{*}\coth\left(\frac{A^{*}\left(H^{*}+h_{s}^{*}\right)}{l^{*}}\right)+\xi_{2}^{*}\coth\left(\frac{B^{*}\left(H^{*}+h_{s}^{*}\right)}{l^{*}}\right)\right)-\left(s^{2}\alpha^{2}M_{o}^{2}\Big/\xi_{3}^{*}\right)}{1-\xi_{1}^{*}\coth\left(\frac{2A^{*}\left(H^{*}+h_{s}^{*}\right)}{l^{*}}\right)+\xi_{2}^{*}\coth\left(\frac{2B^{*}\left(H^{*}+h_{s}^{*}\right)}{l^{*}}\right)}$$

$$\xi_1^* = \frac{2sA^*B^{*2}}{\left(A^{*2}-B^{*2}\right)l^*},\ \xi_2^* = \frac{2sA^{*2}B^*}{\left(A^{*2}-B^{*2}\right)l^*},\xi_3^* = \left(1-\beta+\frac{s^2\alpha^2M_o^2}{M'}\right)$$

The work load is obtained by

$$E(w) = \int_{-2a}^{a}\int_{\frac{-2a+x}{\sqrt{3}}}^{\frac{2a+x}{\sqrt{3}}} E(p)dydx \tag{22}$$

The dimensionless work load is of the form

$$w^* = \frac{\sqrt{3}M_o^2}{60}\left\{\frac{1}{\left(G\left(H^*,\mathrm{s},l^*,\mathrm{M}_o,\mathrm{C}\right)+\frac{\psi M_o^2}{\xi_3^*}\right)}\right\} \tag{23}$$

The time-height relationship is

$$T^* = \int_1^{h_1} W^* dh \tag{24}$$

The dimensionless time - height relationship is

$$T^* = -\frac{\sqrt{3}M_o^2}{60}\int_1^{H_1}\left\{\frac{dh^*}{\left(G\left(H^*,\mathrm{s},l^*,\mathrm{M}_o,\mathrm{C}\right)+\frac{\psi M_o^2}{\xi_3^*}\right)}\right\} \tag{25}$$

**Figure 2**

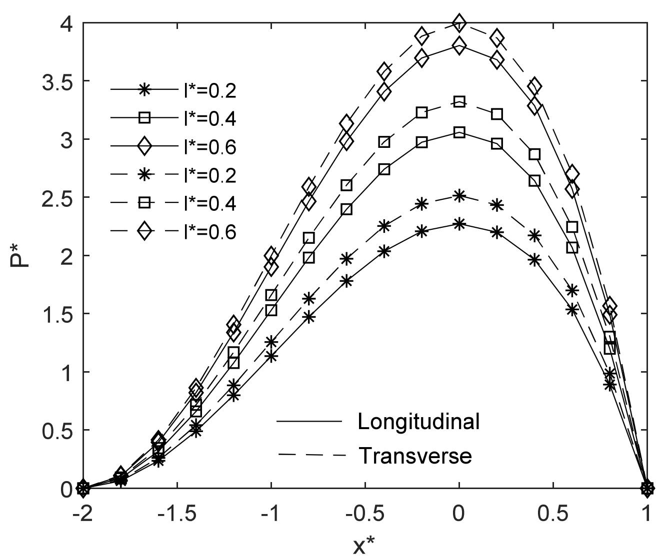


Variation of P* with x*for various values of $l^*$ with $M_o = 1, s = 0.7, \beta = 0.25, \psi = 0.01,\quad \alpha = 0.001, M' = 0.6, H^* = 0.5, \mathrm{C} = 0.3, y = 0$

**Figure 3**

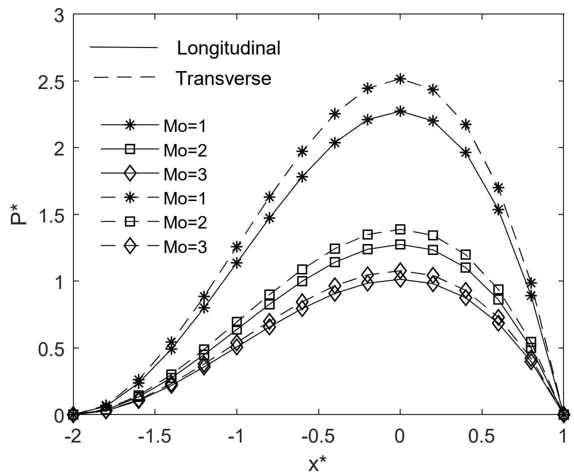


Variation of P* with x*for various values of $M_o$ with $l^* = 0.2, s = 0.7, \beta = 0.25, \psi = 0.01,$ $\alpha = 0.001, y = 0, M' = 0.6, H^* = 0.5, C = 0.3$

**Figure 4**

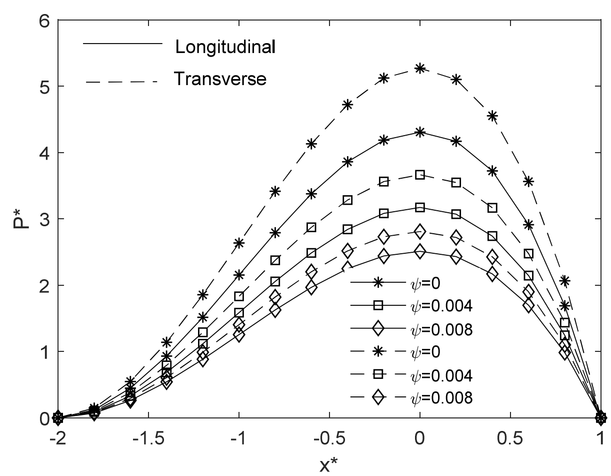


Variation of P* with x*for various values of ψ with $l^* = 0.2, \beta = 0.25, M_o = 1, s = 0.7$ $\alpha = 0.001, y = 0, M' = 0.6, H^* = 0.5, C = 0.3$

**Figure 5**

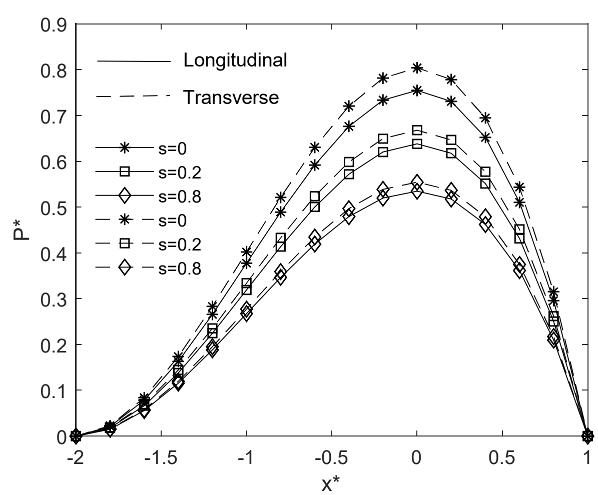


Variation of P* with x*for various values of s with $y = 0, \beta = 0.002, \psi = 0.05, l^* = 0.2, M_o = 1,$ $H^* = 0.8, \alpha = 0.050, M' = 0.1, C = 0.3$

**Figure 6**

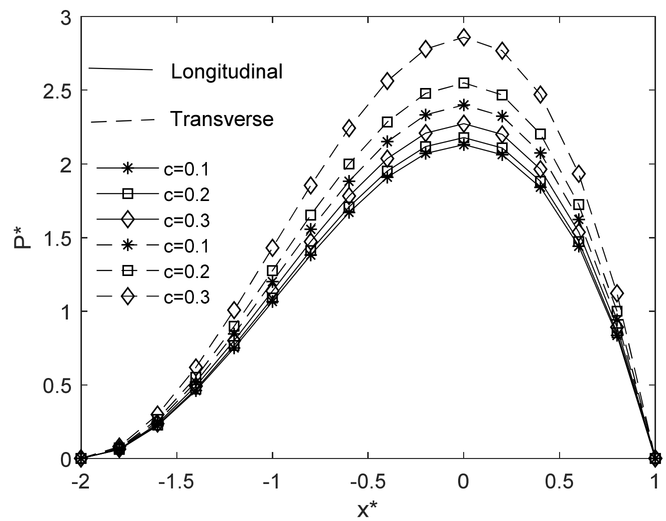


Variation of P* with x*for various values of c with $y=0, l^*=0.2, \beta=0.25, \psi=0.01, M_o=1, \quad \alpha=0.001, M'=0.6, H^*=0.5, s=0.7$

**Figure 7**

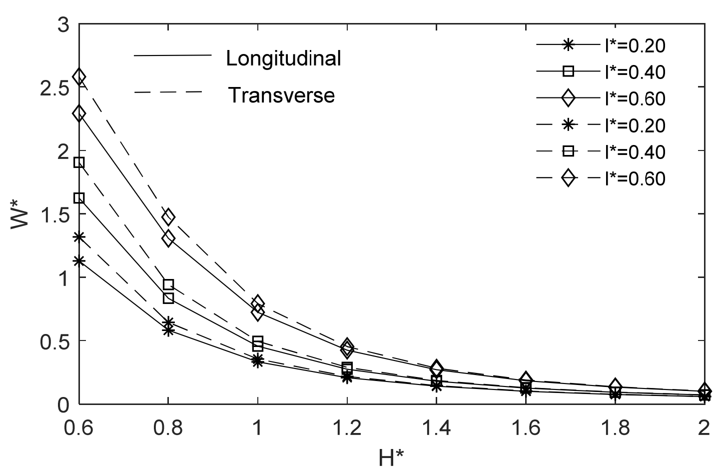


Variation of W* with H* for various values of $l^*$ with $M_o=1, s=0.075, \beta=0.025, \psi=0.0075\ \alpha=0.25, M'=0.7, \mathrm{C}=0.3$

**Figure 8**

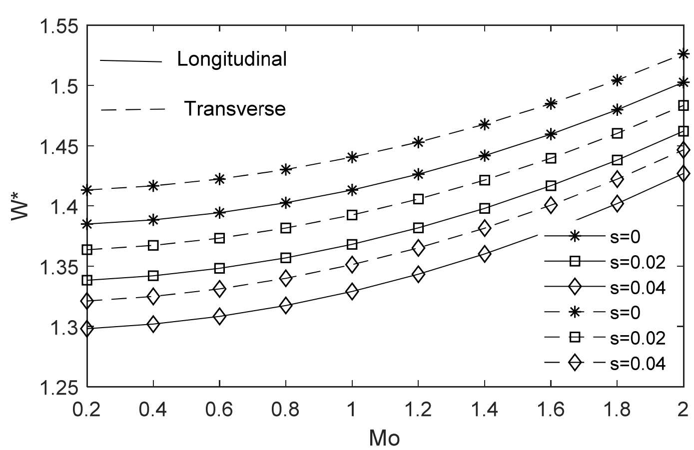


Variation of W* with $M_o$ for various values of s with $H^*=0.5, \beta=0.25, \psi=0.01\ l^*=0.2, \alpha=0.001, M'=0.6, \mathrm{C}=0.1$

**Figure 9**

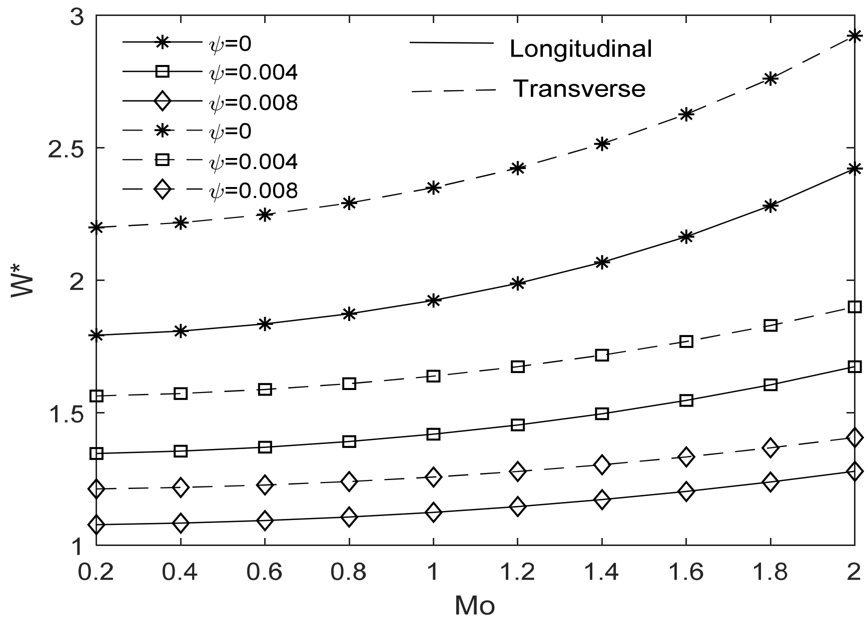


Variation of W* with $M_o$ for various values of ψ with $s = 0.75, H^* = 0.5, \beta = 0.25\ l^* = 0.2, \alpha = 0.01, M' = 0.1, \mathrm{C} = 0.3$

**Figure10**

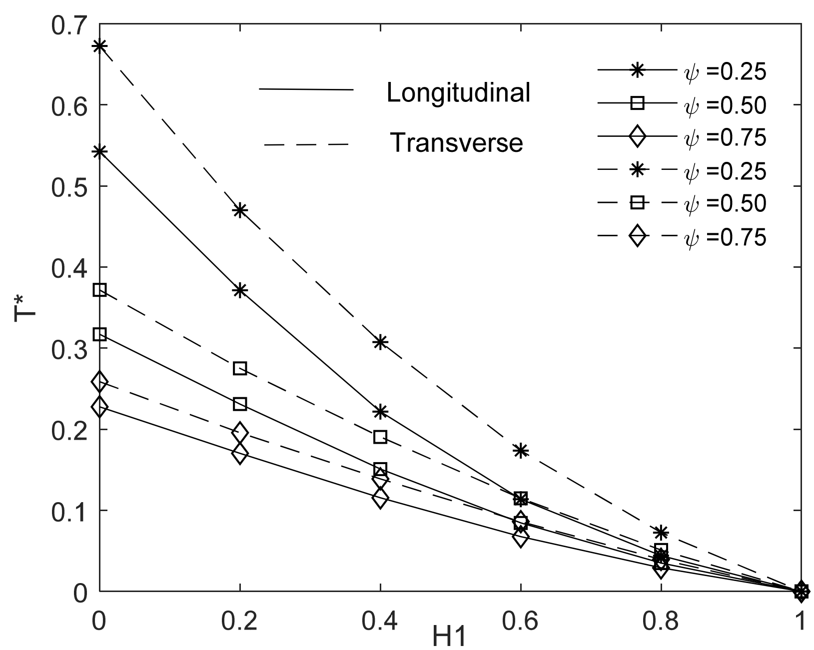


Variation of T* with $H_1$for various values of ψ with $M_0 = 1, s = 0.075, \beta = 0.25\ \alpha = 0.025, l^* = 0.02, M' = 1, \mathrm{C} = 0.3$

## 4. Results and Discussion

Stokes theory [15] is used to analyze the effect of couple stress fluid with MHD and effect of roughness is studied by using Christensen stochastic theory [14]. The dimensionless parameters Hartmann number $M_o$, Permeability parameter ψ, Non-Newtonian couple stress parameter $l^*$, slip velocity s, porosity $M'$ and, roughness parameter C are used to analyze the characteristics of the triangular plates.

The variation of dimensionless pressure p* with the dimensionless co-ordinate x* for various values of $l^*$ are represented in fig.2. In fig 3. the pressure decreases for increasing values of the Hartmann number $M_o$. Fig.4 depicts that as slip velocity increases the pressure decreased. Fig.5 shows that the different values of the permeability parameter ψ with variation of p* with x* for the two types of roughness pattern. When comparing to the solid state (ψ=0) the impact of ψ decreases pressure p*. Fig.6 presents the pressure p* with x* for different roughness parameter c for both longitudinal and transverse pattern.

For various values of $l^*$ in fig.7 shows the variation for dimensionless work load W* along with film height H* for the two roughness patterns. We observed that the load capacity is increased for the increasing values of $l^*$. In fig.8 for the decreasing values of slip velocity s the load carrying capacity increases. Fig9 illustrates the consequence of ψ on the variation of W* with H*. It is noted that the W* decreases for increasing values of ψ.

On considering the different values of ψ there is variation with $H_1$ on dimensionless time T* which is figured out in fig.10. For increasing values of ψ shows that the squeeze film time T* decreased significantly.

## 5. Conclusion

The triangular plates with couple stress fluid using MHD, Surface Roughness, Velocity Slip and porosity the following solutions are obtained from the above given results.

- The Pressure P* is decreased with the increasing slip velocity.
- The rise in couple stress parameter increases the load
- The variation of W* with non-dimensional film thickness H* is shown for various parameters of roughness in both longitudinal and transverse patterns
- Compared to the longitudinal roughness, the transverse roughness seems to be enhanced for all the parameters.

## 6. Nomenclature

u, v, w- velocity parameters in film region

$u^*, v^*, w^*$ - dimensionless velocity parameters in x, y, z directions respectively

$\delta$ - Porous layer thickness

$M'$ = porosity

c - roughness parameter

C- dimensionless roughness parameter $= \frac{c}{h_o}$

H - film thickness

$H^*$ - dimensionless film thickness$= \left(\frac{H}{h_o}\right)$

$\mu$ - Viscosity co-efficient

$l$ – Couple stress parameter $= \sqrt{\left(\frac{\eta}{\mu}\right)}$

$l^*$ -dimensionless couple stress parameter $= \left(\frac{2l}{h_o}\right)$

$B_o$ – Magnetic field

$M_o$ -Hartmann number $= \left( B_o h_o \left( \frac{\sigma}{\mu} \right)^{\frac{1}{2}} \right)$

$\eta$ - Material constant

$\psi$ - Permeability variable $= \frac{k\delta}{h_0^3}$

$\alpha$ – dimensionless slip constant
a-length of the side of the triangle
$\sigma$ - electrically conductivity
$\sigma^*$ - parameter $\left( \sqrt{k} / \alpha \right)$

s- slip parameter $\sigma^* / h_o$

$\sigma = c/3$ is the standard deviation.

K - permeability

$p^*$ - Non-dimensional pressure = $\left\{ \frac{-E(p)h_o^3}{\mu \frac{dh}{dt} \sqrt{3} a^2} \right\}$

$W^*$ - non-dimensional load carrying capacity = $\left\{ \frac{-E(\mathrm{w})h_o^3}{27\mu \frac{dh}{dt} a^4} \right\}$

$T^*$ - non-dimensional time= $\left\{ \frac{E(\mathrm{w})h_o^2 dt}{27\mu a^4} \right\}$

## References

[1] Fathima ST, Naduvinamani NB, Kumar JS, Naganagowda HB 2014 “Derivation of modified Mhd-stochastic Reynolds equation with conducting couple stress fluid on the squeeze film lubrication of porous rough elliptical plates”. *International Journal of Mathematical Archive* 1 pp135-145

[2] Patel KC, Gupta JL. 1983 “Hydrodynamic lubrication of a porous slider bearing with slip velocity”. *Wea*r. Mar 15;85(3):309-17.

[3] N.B. Naduvinamani, B.N. Hanumagowda and SyedaThasneem 2012 Fathima “Combined effects of MHD and surface Roughness on Couple Stress Squeeze film lubrication between porous circular stepped plates” *Tribology International* 56 pp 19-29.

[4] Sundarammal Kesavan., and Santhana Krishnan, N., 2012 “Surface roughness effects on squeeze film behavior in porous transversely triangular plates with couplestress fluid”, *International Journal of Mechanical Engineering and Technology*, 3(2), pp 01-12,

[5] Santhana Krishnan, N., Ali Chamkha., and Sundarammal Kesavan., 2016 “Squeeze film behavior in porous transversely circular stepped plates with a couple stressfluid”, *Engineering Computations, Emerald Publications*, 33(2), pp. 328–343,

[6] Kashinath B. 2013 Magneto hydrodynamic couple stress squeeze film lubrication of triangular plates. *International Journal of Engineering Inventions*.; 3:66-73.

[7] Bujurke NM, Naduvinamani NB and Basti DP 2011 Effect of surface roughness on magneto hydrodynamic squeeze film characteristics between finite rectangular plates *Tribology Internationa*l 7 pp 916-921

[8] Kesavan S, Chamkha A and Krishnan Narayanan S 2014 "Magnetohydrodynamic (MHD squeeze film Characteristics between finite porous parallel rectangular plates with surface roughness *International Journal* of *Numerical Methods for Heat & Fluid Flow* 2 pp1595-609

[9] Fathima ST, Naduvinamani NB, Marulappa SH. 2012 "Hydromagnetic Squeeze Films between Porous Rectangular Plates with Couple stress Fluids". *Tribology Online*. Nov 30;7(4):258-66.

[10] Kudenatti RB, Murulidhara N and Patil HP 2013 "Numerical solution of the MHD Reynolds equation for squeeze-film lubrication between porous and rough rectangular plates". *Tribology*

[11] Basti DP 2013 "Effect of surface roughness and couple stresses on squeeze films between curved annular plates" *Tribology* 7**.**

[12] Naduvinamani NB, Siddangouda A 2007 "Effect of surface roughness on the hydrodynamic lubrication of porous step-slider bearings with couple stress fluids" *Tribology International* pp780-93

[13] Sparrow EM, Beavers GS and Hwang IT 1972 "Effect of velocity slip on porous walled squeeze films" *Journal of Lubrication Technology* 3 pp 260-44.

[14] Christensen H 1969 "Stochastic models for hydrodynamic lubrication of rough surfaces" *Proceedings of the Institution of Mechanical Engineers* 1 pp1013-26.

[15] Stokes V.K. 1966 "Couple stress in fluids", *The physics of fluids* vol 9 pp 1709-15

[16] Cameron A. 1981" Basic lubrication theory". *3rd Ed. New York John Wiley & Sons*